# The Effects of Temperature on Hydrodynamic Interaction of Sedimenting Semi-Flexible Brownian Fibres

**N Hajaliakbari[1], D Head[1] and O Harlen[2]**
[1] School of Computer Science, Faculty of Engineering and Physical Science, University of Leeds, Leeds, UK
[2] School of Mathematics, Faculty of Engineering and Physical Science, University of Leeds, Leeds, UK

**Keywords: Rotne-Prager-Yamakawa Singularities, Hydrodynamic Interactions, Brownian Motion, Sedimentation, Trimer Model**

**Abstract.** Some processes for material or composite making, such as papermaking or fibre-reinforced composites, involve the sedimentation of semi-flexible fibres due to gravitational forces. A precise numerical tool that can evaluate the hydrodynamic interactions among these fibres would be useful in the design of novel fibre materials. In this research study, the Rotger-Prager-Yamakawa (RPY) singularity representation is used to simulate the hydrodynamic and thermal fluctuations between semi-flexible fibres with results compared to predictions of a simpler trimer model (Oseen approximation). For a pair of sedimenting semi-flexible fibres, it is found that by an increase in temperature, the curvature also increases due to the decrease in hydrodynamic interactions compared to thermal fluctuations at a constant bending stiffness. Also, the final bending angle (curvature) was proportional to elastogravitational number, as predicted by both models. Finally, it was observed that the early rate of rotation varied inversely with the nondimensionalised shortest distance between end-to-end of fibres.

## 1. Introduction

Sedimentation is a process that arises in the production of materials such as paper, fibre-reinforced composites etc. Depending upon the material properties and physical length scales, thermal fluctuations (Brownian motion), as well as internal elasticity, viscous and gravitational forces, can affect the dynamics. In addition, hydrodynamic interactions between fibres become comparable to other forces when the neighbouring fibres are close to each other.

The conformation of a single semi-flexible fibre sedimenting within a viscous fluid has been extensively studied. In the absence of Brownian motion, the steady state configuration of a single fibre falls into one of three different regimes depending on the its stiffness relative to gravity [1]. Cunha et al. [2] considered the effects of Brownian fluctuations and showed that these led to deformations around the steady state configuration for an equivalent non-Brownian fibre. Along with some experiments, a numerical tool was also employed which revealed a W-like configuration for highly flexible fibres that had not been previously reported in the experiments. The fibres were modelled using Slender Body Theory, a method based on a distribution of singular forces along a cylindrical object. The results predicted that the effects of the initial configuration of a flexible filament are significant. In fact, compared to a horizontally aligned fibre, a vertically aligned fibre is more susceptible to buckling [3].

In addition to these studies of single fibres some research studies have been done on understanding the details on the sedimentation of multiple fibres. They primarily focused on studying the hydrodynamic interactions among a cluster of settling fibres. For instance, Tornberg and Gustavsson [4] introduced a numerical tool to simulate non-Brownian rigid fibres, which was based on the non-local slender body approximation. The results showed that the average velocity of an assembly of fibres is higher than an individual fibre.

Others have simplified the problem by studying interactions between a small number of fibres. Llopis et al. analysed the motion of a pair of flexible fibres in three initial configurations [5]. The fibres eventually collided with each other when they were initially close to each other. In this study the fibres were modelled as a string of connected spheres rather than as a continuous cylinder. Very recently, Maxian and Donev studied the hydrodynamic interactions for a pair and a collection of Brownian fibres

[6]. It was shown that the fibres approach each other as the hydrodynamic interactions is strong in comparison to Brownian motion. However, that research work was limited to only one set of parameters. In addition, no results were reported on the end-to-end vertical distance and curvature changes for fibres. To the authors' knowledge, there is no systematic research study on the effects of temperature (Brownian motions) on end-to-end vertical distance and curvature of semiflexible fibres with consideration of full hydrodynamic interactions during sedimentation.

## 2. Methodology

### *2.1. Rotne-Prager-Yamakawa (RPY) kernels (numerical model)*

In a numerical tool, developed by Maxian et al. [7, 8], Rotne-Prager-Yamakawa (RPY) kernels were used to study the full hydrodynamic interactions among sedimenting Brownian fibres. This ensures that the hydrodynamic mobility matrix is symmetric positive definite, which is required for the implementation of Brownian motion.

To mathematically describe the fibre profile, a fibre is modelled as a series of $m_x$ connected blob-links (rigid rods). This can be discretised into $m$ points (grids), by the use of type 2 Chebyshev polynomials ($m$ is the number of tangent vectors ( $m_x$) on type 1 Chebyshev polynomials plus one) representing the fibre centreline. The Chebyshev points and tangent vectors, which describe the discretised fibre centreline, have been illustrated in Figure 1. As can be clearly seen, these points and vectors are not uniformly distributed.

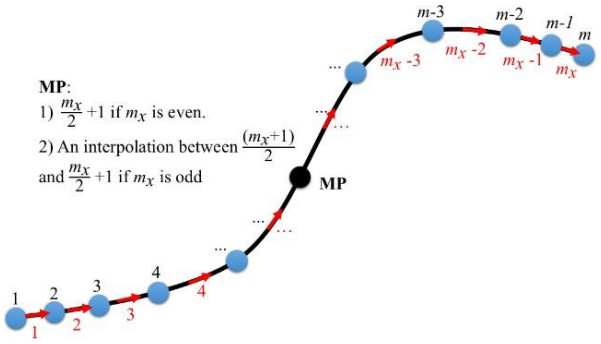


Figure 1. The configuration of a discretised fibre described by Chebyshev points (blue and black solid circles) and tangent vectors (red arrows). The solid black line represents the continuous profile of the fibre.

The position of the fibre points (blue and black solid circles in Figure 1) $\mathbf{X}$ can be obtained by the integration operator $\chi$,

$$\mathbf{X} = \chi\left(\boldsymbol{\tau}, \mathbf{X}_{MP}\right) \tag{1}$$

where $\boldsymbol{\tau}$ and $\mathbf{X}_{MP}$ are the tangent vectors (red arrows in Figure 1) and position of the midpoint (the solid black circle in Figure 1), respectively.

In the quasi-steady or overdamped regime, for which the hydrodynamics rapidly relaxes relative to the time-scale of microstructure motions, the dynamics of the fibre is given by the Ito-Langevin equation in terms of $\mathbf{X}$ , expressed as [8, 9]

$$\partial_t \mathbf{X} = -\mathbf{M}\,\mathbf{L}\,\mathbf{X} + k_B T\,\partial_X \mathbf{M} + \sqrt{2k_B T}\,\mathbf{M}^{\frac{1}{2}}\,\mathbf{W}(t). \tag{2}$$

The first term on the right-hand side of equation (2) arises from the deterministic dynamics (saddle point system) and includes the elastic and hydrodynamic forces, while the second and third terms correspond to the drift and noise terms, respectively. Here, $\mathbf{W}(t)$ is a vector of i.i.d white-noise processes (the formal derivatives of Brownian motion). The mobility matrix $\mathbf{M}$ must satisfy the fluctuation-dissipation relation [8], that is,

$$\mathbf{M}^{\frac{1}{2}}(\mathbf{M}^{\frac{1}{2}})^{T} = \mathbf{M}. \tag{3}$$

It is worth noting that the matrix $\mathbf{M}^{\frac{1}{2}}$ is not unique and only needs to satisfy the above relation.

*2.1.1. Mobility matrix*

The hydrodynamic interactions are encapsulated by the mobility matrix **M**. Although this is a dense matrix, it can be divided into local and nonlocal parts,

$$\mathbf{M} = \mathbf{M}^{L} + \mathbf{M}^{NL}. \tag{4}$$

Here, $\mathbf{M}^{L}$ is a block-diagonal matrix which represents the hydrodynamics of a fibre on itself (local or self terms). $\mathbf{M}^{NL}$ represents the contribution of all other fibres to hydrodynamics of that fibre (nonlocal hydrodynamic interaction). The Rotne-Prager-Yamakawa singularities are used to evaluate both local and nonlocal terms, depending on where the forces are imposed and the velocities are calculated. This division (local and nonlocal effects) leads to the easier algebraic operation and a less computationally expensive procedure.

In general, the mobility matrix on each point of a fibre is evaluated by the following equation,

$$\mathbf{M}^{NL}(\mathbf{x}, \mathbf{y}) = \frac{1}{8\pi\mu} \begin{cases} \left(\frac{\boldsymbol{I} + \hat{\boldsymbol{R}}\hat{\boldsymbol{R}}}{R} + \frac{2\hat{a}^2}{3}\frac{\boldsymbol{I} - 3\hat{\boldsymbol{R}}\hat{\boldsymbol{R}}}{R^3}\right) & R > 2\hat{a} \\ \left(\left[\frac{4}{3\hat{a}} - \frac{3R}{8\hat{a}^2}\right]\boldsymbol{I} + \frac{R}{8\hat{a}^2}\hat{\boldsymbol{R}}\hat{\boldsymbol{R}}\right) & R \le 2\hat{a} \end{cases} \tag{5}$$

where $\mathbf{R} = \mathbf{x} - \mathbf{y}$, $R = \|\mathbf{R}\|$, $\hat{\mathbf{R}} = \mathbf{R} / \|\mathbf{R}\|$, and $\hat{\mathbf{R}}\hat{\mathbf{R}}$ are the distance vector, distance vector length, normalized distance vector and outer product of $\hat{\mathbf{R}}$ with itself, respectively. The parameter $\hat{a} \approx 1.12\,a$ is the regularized singularity radius with $a$ the radius of the fibre. A two-step (two major steps) time integrator for evaluation of the motion of Brownian fibres has been used here [8]. Further elaborations regarding this numerical model can be found in the literature [6-8].

*2.2. Trimer model*

For a simple model of early fibre dynamics, we consider a trimer representation in which each fibre is modelled by three non-overlapping beads with all forces acting at bead centres, as shown in Figure 2. This follows Llopis et al. [5] for the geometry here and with the inclusion of explicit bending forces.

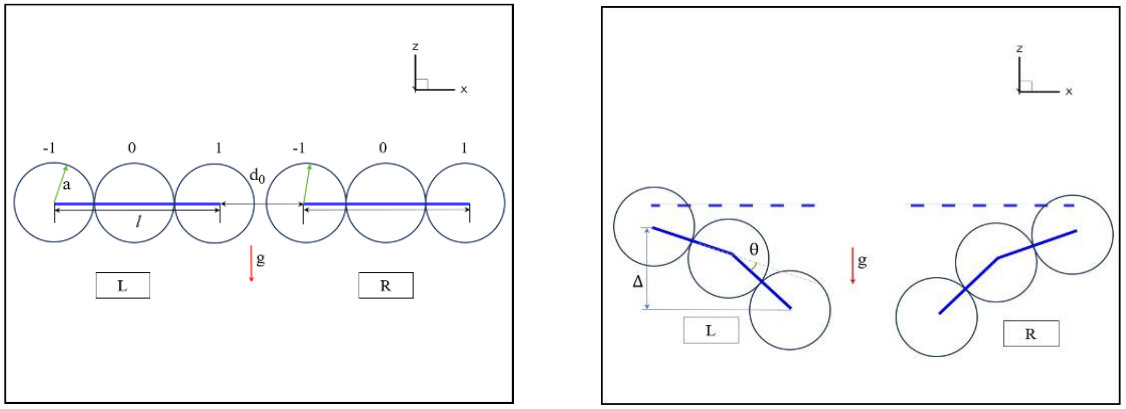


Figure 2. Some parameters written in subscript or superscript for a trimer model (left image) and a couple of degrees of freedom defined for its deformation (right image)

The Oseen approximation is then used to calculate the hydrodynamic interactions so that the velocity for each bead is given

$$\mathbf{v}_i\mathbf{e}_z = \frac{1}{8\pi\eta}\sum_{j\neq i}\frac{1+\mathbf{e}_{ik}\mathbf{e}_{ij}}{r_{ij}}\mathbf{F}_j \tag{6}$$

By further approximating that the fibres remain close to their initial configurations, we can obtain the evolution equations for the vertical distance between the fibre ends Δ and bending angle $\theta$ as functions of fibre length, $l$, stiffness $k$, weight $W$ and separation $d$ as

$$\frac{d\Delta(t)}{dt} = \frac{l}{4\pi\eta A}\{[l(l+4d)+2d^2]W+12k\theta(t)\} \tag{7}$$

$$\frac{d\theta(t)}{dt} = \frac{1}{6\pi\eta l^2}\left(1-\frac{3l^3}{B}[l(l+2d)+d^2]\right)W-\frac{k}{\pi\eta l^4}\left(18+\frac{l^5}{6B}\right)\theta(t) \tag{8}$$

The full solutions for these equations are given by

$$\theta(t) = \theta^{\infty}\,(1 - e^{-t/t_0}) \tag{9}$$

$$t_0 = \frac{\pi\eta l^4}{k(18+l^5/6B)} \tag{10}$$

$$\theta^{\infty} = \frac{Wl^2}{k}\left(\frac{B-3l^3[l(l+2d)+d^2]}{108B+l^5}\right) \tag{11}$$

$$\Delta(t) = \frac{1}{4\pi\eta A}\{[l(l+4d)+2d^2]W+12k\theta^{\infty}\}t+\frac{3kl t_0\theta^{\infty}}{\pi\eta A}\left(e^{-\frac{t}{t_0}}-1\right). \tag{12}$$

Here, $A$ and $B$ are polynomials of $l$ and $d$, $A=d(l+2d)(3l+2d)(2l+d)$ and $B=d(l+2d)(l+d)(3l+2d)(2l+d)$, respectively. The bending angle reaches its final value ($\theta^{\infty}$) (a plateau), as discussed below.

## 3. Results

To capture basic physical phenomena related to hydrodynamic interactions, a pair of sedimenting semiflexible Brownian fibres, which are initially collinear, is considered. The physical behaviour of this system can be described by a set of nondimensional parameters: the elastogravitational number ($B^* = \frac{\Delta\rho g l^3}{k}$), the nondimensional bending elasticity ($K^* = \frac{l_p}{l} = \frac{k}{(k_B T)l}$), the gravitational Peclet number ($Pe_g = \frac{2\pi a^3\Delta\rho g l}{3k_B T}$), the nondimensional distance, i.e., the ratio of the initial shortest distance between end-to-end of collinear fibres and the fibre length ($D^*$), the aspect ratio of the fibre ($\epsilon = \frac{a}{l}$) (the ratio of fibre radius to its length), and the nondimensional simulation time ($T^* = \frac{t}{\tau} = \frac{t\mu l}{\Delta\rho g}$), where $l$, $g$, k, $k_B$, T, $\Delta\rho$, $a$, $l_p$, t and $d_0$ are the fibre length, gravitational acceleration constant, bending stiffness of fibre, Boltzmann constant, temperature, the difference between the density of fibre and fluid, fibre radius, persistence length, time and the initial shortest end-to-end distance between a pair of collinear fibres, respectively. A schematic description of these parameters defined for a pair in collinear configuration has been illustrated in Figure 3 (left). Note that B*, K* and $Pe_g$ are not independent of each other.

As an initial study of the effect of thermal fluctuation the parameters $B^*$, $D^*$ and $\epsilon$ were set to be 2.0, 0.5 and 0.0046, respectively with $K^* = 5\text{x}10^6$. As the pair of fibres starts to sediment, they rotate in opposite directions due to hydrodynamic interactions and then drift towards each other; see the snapshot at $T^* = 700$ in Figure 3 (right). They subsequently collide with each other (snapshot at $T^* = 1370$) then separate from each other and become horizontal (snapshot at $T^* = 2340$) before repeating the cycle. Since these fibres are quite stiff, they bend into a shallow U shape. The corresponding values of the curvature are shown in the right-hand image in Figure 3.

As the fibres rotate, there is first a decrease and then an increase in curvature up to the point of collision and then a subsequent decrease and increase as the fibres become horizontal again. To examine the effects of thermal fluctuations, $K^*$ was varied from $5x10^8$ down to $5x10^5$ at a fixed value of the $B^*$. For large values of $K^* > 5x10^7$ thermal fluctuations have a negligible effect on the fibre motion; however, as the value of $K^*$ decreases, we see an increase in curvature due to thermal fluctuations that are superimposed on the interactive motion. For $K^* < 10^5$ thermal fluctuations dominate.

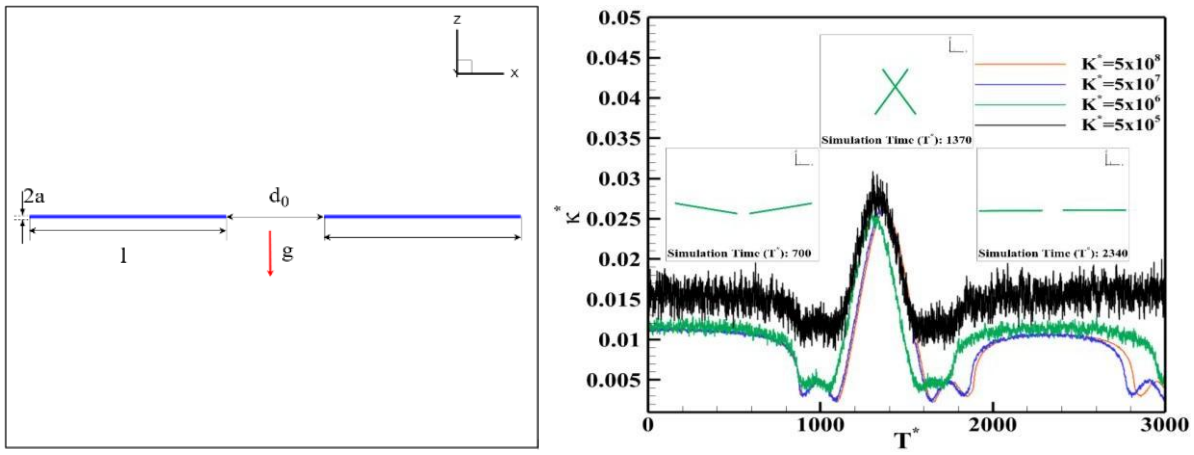


Figure 3. A representation of physical parameters used for description of initially collinear configuration of a pair of flexible fibre (left image) and the transition of curvature magnitude $\kappa^*$ from hot ($K^*=5x10^5$) to cold ($K^*=5x10^8$) case studies (right image)

To assess the effects of varying the elastogravitational number $B^*$, we now focus on the case $K^*=5x10^8$ where thermal fluctuations are negligible, and compare the simulation results with the analytical solutions obtained from the trimer model. The results for both have been illustrated in Figure 4 and show that the bending angle during the early time plateau is proportional the elastogravitational number ($B^*$), and therefore inverse proportional to the fibre bending modulus ($k$), as a consequence of intra-fibre hydrodynamic interactions (Figure 4 (top)). There is also a weak change for close fibres ($D^*=0.1$) as a consequence of the enhanced hydrodynamic interactions. The trimer model exhibits similar trends but significantly over-estimates both the final bending angle ($\theta^\infty$) and the variation with $D^*$. This can be explained by the artificial localisation of forces at bead centres, resulting in much stronger hydrodynamic interactions for nearby trimers compared to the Rotne-Prager-Yamakawa singularities (numerical model), for which the forces are uniformly distributed along the fibre. This decreases the torque over the fibre and therefore the final bending angle would also decrease.

The rotation of the fibres can be estimated as the ratio of the end-to-end vertical distance $\Delta$ and time t at the peak of $\Delta$. As seen in Figure 4 (bottom), this ratio decreases for higher $D^*$ as the fibres tend to sediment more horizontally (magenta hollow squares), as expected since the hydrodynamic interactions are weaker at greater distances. The trimer model (black solid line) captures this trend but fails to reproduce the weak variation with fibre stiffness evident in Figure 4 (bottom). This may be in part due to the retraction of fibre ends in the full numerical model, which acts to increase the separation between nearby fibre points, thereby reducing the strength of the hydrodynamic interactions; indeed, this variation is most pronounced for the softest fibres (highest $B^*$) for which the lateral retraction should be most pronounced. The trimer model assumes fibre configurations remain horizontal to first order and only vertical motion is possible, so it cannot hope to capture this effect.

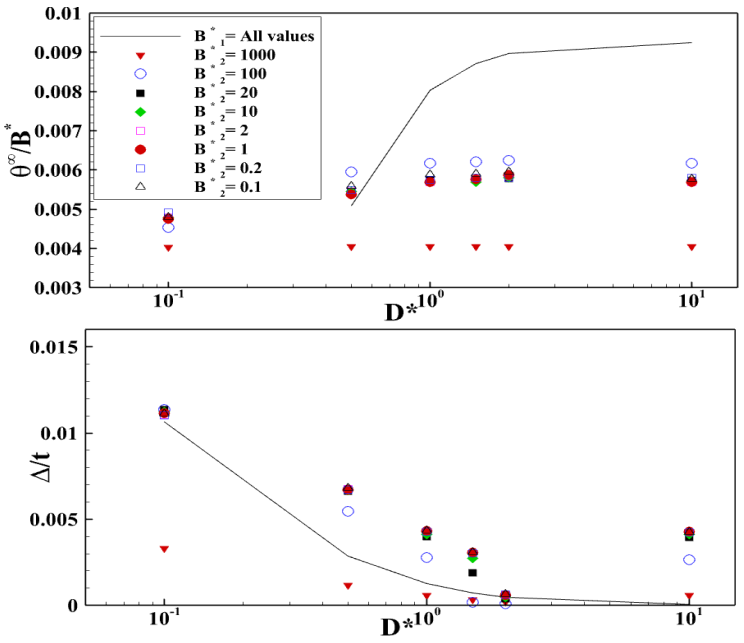


Figure 4. The changes in the final bending angle $\theta^{\infty}$ (or curvature $\kappa^{*}$) and the ratio of the end-to-end vertical distance and time ($\Delta/t$) for one fibre. The subscript 1 and 2 indicate the results from the trimer and numerical models, consequently.

## 4. Conclusion

Based on the results, it can be concluded that, for a pair of sedimenting collinear fibres, the curvature increases due to the fact that the thermal fluctuations are superimposed on the interactive motion of fibres, and furthermore that the final bending angle is proportionally related to elastogravitational number. The trimer model permits a full analytical solution in the athermal limit that reproduces the general trends but significantly overestimates the role of hydrodynamic interactions, essentially because trimers have a disproportionate mass at their ends compared to the cylindrical fibres; it also assumes near-horizontal configurations throughout sedimentation.

## 5. References

[1] Marchetti B, Raspa V, Lindner A, Du Roure O, Bergougnoux L, Guazzelli E, et al. Deformation of a flexible fiber settling in a quiescent viscous fluid. Physical Review Fluids. 2018;3(10):104102.
[2] Cunha LH, Zhao J, MacKintosh FC, Biswal SL. Settling dynamics of Brownian chains in viscous fluids. Physical Review Fluids. 2022;7(3):034303.
[3] Li L, Manikantan H, Saintillan D, Spagnolie SE. The sedimentation of flexible filaments. Journal of Fluid Mechanics. 2013;735:705-36.
[4] Gustavsson K, Tornberg A-K. Gravity induced sedimentation of slender fibers. Physics of fluids. 2009;21(12).
[5] Llopis I, Pagonabarraga I, Cosentino Lagomarsino M, Lowe CP. Sedimentation of pairs of hydrodynamically interacting semiflexible filaments. Physical Review E—Statistical, Nonlinear, and Soft Matter Physics. 2007;76(6):061901.
[6] Maxian O, Donev A. A simulation platform for slender, semiflexible, and inextensible fibers with Brownian hydrodynamics and steric repulsion. arXiv preprint arXiv:240815913. 2024.
[7] Maxian O, Donev A, Mogilner A. Interplay between Brownian motion and cross-linking controls bundling dynamics in actin networks. Biophysical journal. 2022;121(7):1230-45.
[8] Maxian O. Hydrodynamics of transiently cross-linked actin networks: theory, numerics, and emergent behaviors: New York University; 2023.
[9] Peláez RP. Complex fluids in the Gpu era: Algorithms and simulations: Universidad Autónoma de Madrid; 2022.